Progress in Neurobiology 236 (2024) 102611

Contents lists available at ScienceDirect

Progress in Neurobiology

journal homepage: www.elsevier.com/locate/pneurobio

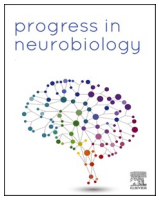

Mixed selectivity in monkey anterior intraparietal area during visual and motor processes

Monica Maranesi *, Marco Lanzilotto, Edoardo Arcuri, Luca Bonini

Department of Medicine and Surgery, University of Parma, Parma 43125, Italy

ARTICLE INFO

Keywords:
Grasping
Object coding
Action observation
Mirror neuron

ABSTRACT

Classical studies suggest that the anterior intraparietal area (AIP) contributes to the encoding of specific information such as objects and actions of self and others, through a variety of neuronal classes, such as canonical, motor and mirror neurons. However, these studies typically focused on a single variable, leaving it unclear whether distinct sets of AIP neurons encode a single or multiple sources of information and how multimodal coding emerges. Here, we chronically recorded monkey AIP neurons in a variety of tasks and conditions classically employed in separate experiments. Most cells exhibited mixed selectivity for observed objects, executed actions, and observed actions, enhanced when this information came from the monkey's peripersonal working space. In contrast with the classical view, our findings indicate that multimodal coding emerges in AIP from partially-mixed selectivity of individual neurons for a variety of information relevant for planning actions directed to both physical objects and other subjects.

1. Introduction

The posterior parietal cortex underwent considerable expansion during phylogeny (Bruner, 2018), hosting uniquely human lateralized functions added to a basic anatomo-functional organization largely shared among primates (Orban, 2016). Deficits as diverse as limb apraxia (Buxbaum and Randerath, 2018) and spatial neglect (Vallar and Calzolari, 2018) occur in humans following left and right inferior parietal lesions, respectively; furthermore, reversible disruption of the human left inferior parietal lobule impairs perceptual functions such as the readout of other's intention based on observed actions' kinematics (Patri et al., 2020). Thus, high order spatial and perceptual functions instrumental to planning and organizing actions seem to represent the evolutionary preserved coding principle of the posterior parietal cortex (Kaas et al., 2018; Orban et al., 2021a).

Among the multiplicity of posterior parietal areas, the anterior intraparietal area (AIP) has been subject to increasing interest in the last thirty years in both human and monkey neuroscientific literature because it constitutes a convergence node for multiple visual and somatosensory information about the physical properties of objects and other's observed actions, as well as of motor signals and higher order information from the frontal cortex (Borra et al., 2008; Lanzilotto et al., 2019). However, the coding principles underlying such a variety of afferents and multiplicity of functions remain poorly understood. The prevailing, textbook view on this issue (Kandel et al., 2021) emphasizes the relevance of distinct neural categories in AIP: motor neurons (discharging only during grasping of objects in the dark), visual neurons (discharging during object presentation and/or during the observation of self or other's actions), canonical neurons (discharging during visual presentation and the subsequent grasping of objects), and mirror neurons (discharging during grasping execution and observation). Each of these categories would be dedicated to the encoding of either objects or actions in a purely motor, purely visual, or visual and motor format.

However, this picture derives from neurophysiological studies of area AIP that typically employed a single task to shed light on a single, or a few, specific properties at a time, such as visual contextual cues for grasping (Baumann et al., 2009), object fragments (Romero et al., 2014; Romero and Janssen, 2016), object shapes in 2d (Romero et al., 2012) and 3d (Theys et al., 2012, 2013; Verhoef et al., 2015), graspable objects' visual shape, size, and orientation (Murata et al., 1996, 2000; Schaffelhofer and Scherberger, 2016), spatial signals (Lehmann and Scherberger, 2013), grip type (Schaffelhofer and Scherberger, 2016; Sakata et al., 1995), grasp force (Intveld et al., 2018), and one's own hand visual feedback or observed actions of others (Lanzilotto et al., 2019, 2020; Pani et al., 2014; Maeda et al., 2015; Ferroni et al., 2021). A similarly distributed coding of different information across a variety of

* Corresponding author.
E-mail address: monica.maranesi@unipr.it (M. Maranesi).

https://doi.org/10.1016/j.pneurobio.2024.102611
Received 17 November 2023; Received in revised form 29 February 2024; Accepted 8 April 2024
Available online 10 April 2024

neuronal categories was also considered a hallmark feature of the premotor cortex (Rizzolatti and Luppino, 2001), but more recent evidence obtained by testing individual cells with a variety of execution and observation tasks (Bonini et al., 2014) revealed that single premotor neurons exhibit highly multimodal coding of sensory and motor information regarding both objects and self/other actions. Interestingly, a unifying principle underlying the premotor coding of observed objects and actions appears to be their pragmatic relevance for the observer: indeed, when a transparent plastic barrier is interposed between the observer and the observed stimuli (Barrier condition), visual responses to both graspable objects (Bonini et al., 2014; Lanzilotto et al., 2016) and the observed actions of others (Caggiano et al., 2009) are strongly modulated, even if the retinal images of the stimuli remain unchanged. This prompted the idea that action plans afforded by environmental stimuli may derive from the activation of the same premotor neurons encoding manipulative actions while observing 3d objects and the actions of others (Maranesi et al., 2014; Bonini et al., 2022), likely involving the parietal cortex as a crucial source of visual information for affordance extraction (Orban et al., 2021a, 2021b).

Therefore, the main emerging question is whether in AIP multimodal coding emerges by means of distinct sets of intermingled neurons, each dedicated to the encoding of a specific type of information (e.g. objects or actions) or, instead, a non-categorically distinct set of neurons with mixed selectivity for multiple variables. To distinguish between these alternative hypotheses, we leveraged chronic recording of single neuron activity from area AIP in two monkeys while they performed a Go/No-go motor task, observed it performed by an experimenter (Bonini et al., 2014; Maranesi et al., 2015), and when they performed an observation task with video stimuli. Our findings allowed us to shed light on the relationships between the multimodal encoding of information in AIP from the single neuron to the neural population level. Furthermore, control experiments carried out by leveraging the Barrier condition revealed that a substantial fraction of AIP neurons reflects a pragmatic coding of visual information that can be relevant for the planning of ethologically relevant actions.

2. Results

We isolated 134 single neurons (n = 110 from Mk1 and n = 24 from Mk2) from extracellular recordings carried out at different locations along the anteroposterior extent of area AIP of two monkeys (Fig. 1A). The exact location and connectional fingerprint of the investigated sectors in both monkeys have been described in detail in a previous neurophysiological study carried out with the same chronic implants (Lanzilotto et al., 2019). During the recordings, the monkeys performed, in different blocks, 1) a visuomotor Go/No-Go task (VMT, Fig. 1B), 2) an observation task in which they observed from a subjective viewpoint an experimenter doing the VMT in their stead in their peripersonal space (OTp, Fig. 1C), 3) an observation task in which they observed from a lateral viewpoint an experimenter doing the VMT in their extrapersonal space (OTe, Fig. 1D), 4) an observation task in which they observed on a screen goal-directed or pantomimed hand actions and isolated objects, in either static frames or dynamic videos (OTv, Fig. 1E). During the observation tasks, monkeys were required to keep their hand still on the starting position and to keep fixation all along the trial. The objects target of the monkey or the experimenter's action were a small sphere (to be grasped with a precision grip) and a big one (to be grasped with a whole-hand prehension). Importantly, the temporal sequence of events in the VMT, OTp, and OTe was the same (Fig. 1F), whereas OTv consisted in the presentation of goal directed or pantomimed actions, either

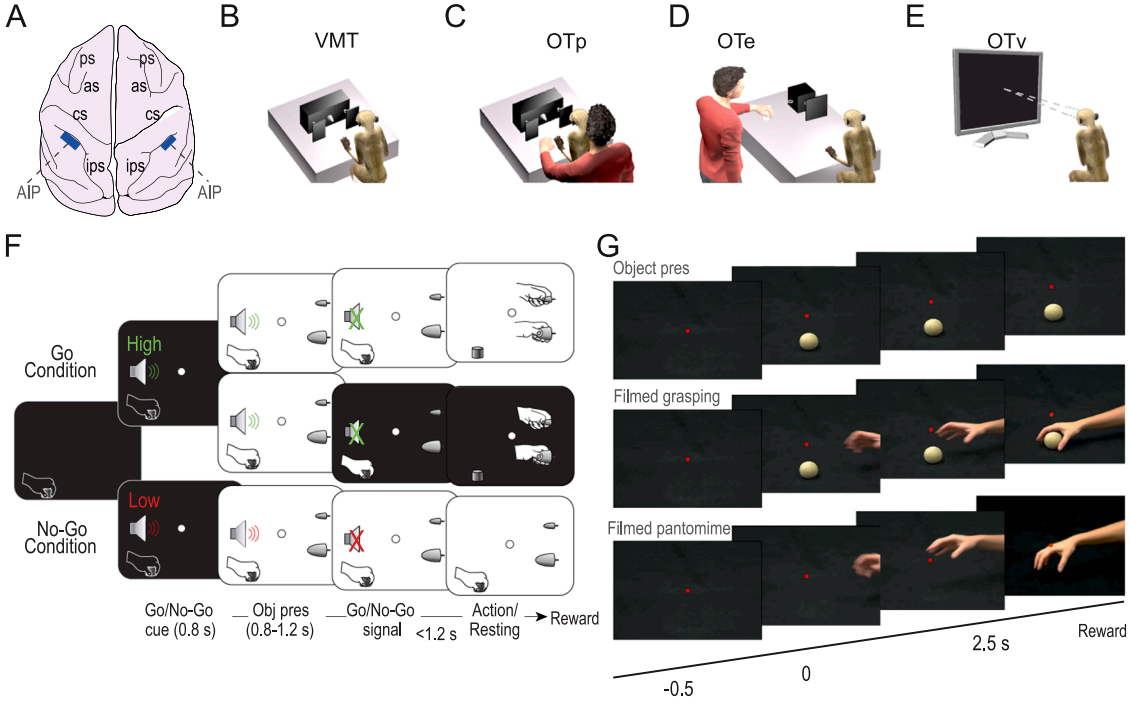

Fig. 1. Recorded region and behavioral tasks. (A) Schematic reconstruction of the recorded regions in the two animals reported on Mk1 brain. As, arcuate sulcus; cs, central sulcus; Ips, intraparietal sulcus; ps, principal sulcus. (B) Behavioral setting for the execution of the visuomotor task (VMT). (C) Behavioral setting for the observation task in the monkey's peripersonal space (OTp). (D) Behavioral setting for the observation task in the monkey's extrapersonal space (OTe). (E) Behavioral setting for the observation task with video stimuli (OTv). (F) Temporal sequence of events of the Go/No-Go visuomotor task. The monkey starts with its hand in a fixed position. The onset of central fixation in the position where the object will be presented triggers a Go/No-Go auditory cue (high-/low-frequency sound, respectively). Following a variable delay after object presentation, the end of the sound (Go/No-Go signal) instructs the monkey to reach and grasp the visually presented object or to remain still until the end of the trial to obtain the reward. The different types of trials (Go/No-Go and object type) within VMT and OT blocks were presented in a randomized order. (G) Temporal sequence of events in the OTe. From the onset of central fixation point to the end of the trial, monkey has to keep fixation and the hand still at the starting position.

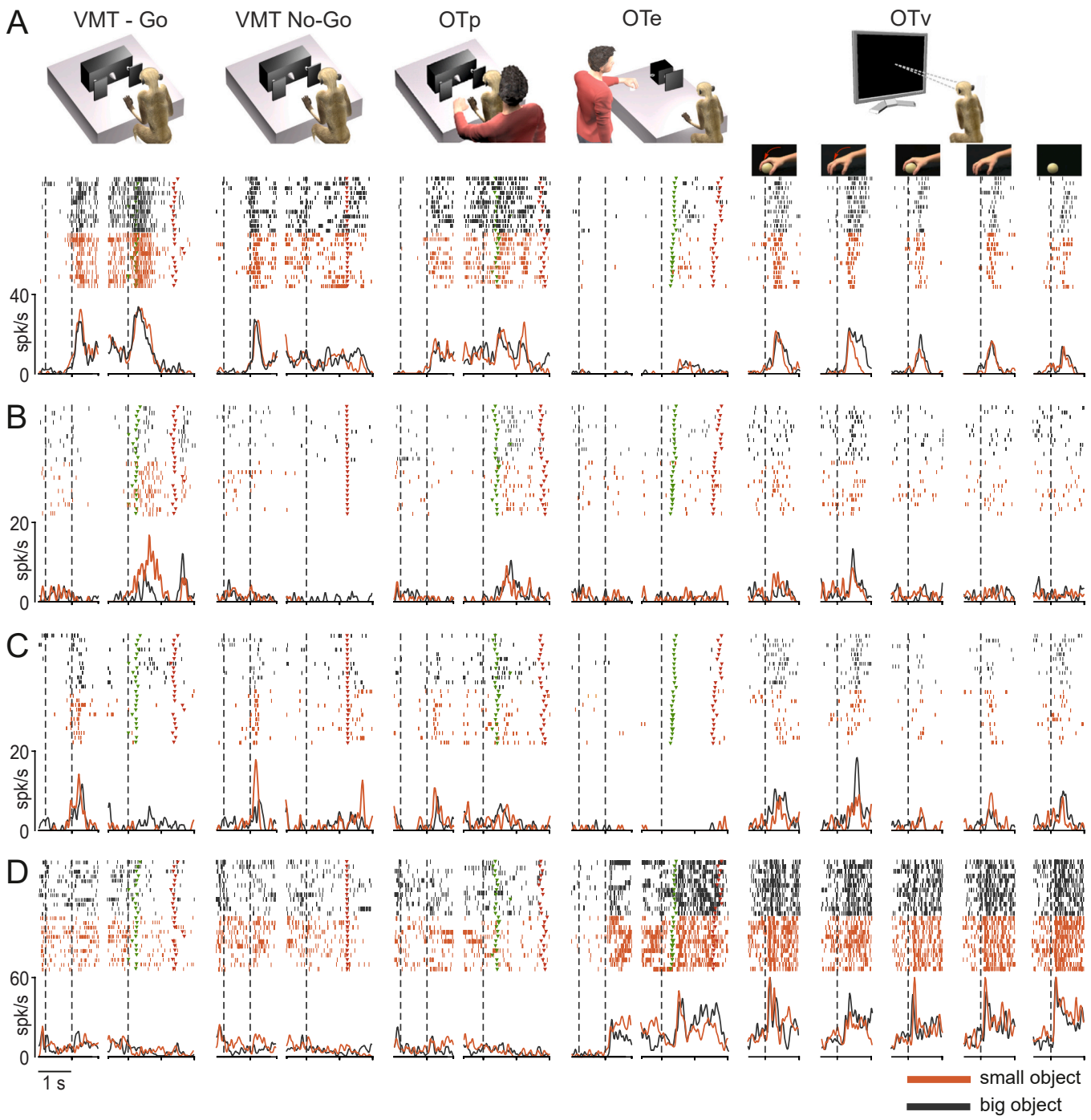

Fig. 2. Examples of AIP neurons simultaneously recorded in all tasks. (A) Schematic representation of each task and example neuron classified as visuomotor in the VMT. VMT Go, Go condition of the VMT in the dark; VMT No-go, No-Go condition of the VMT; OTp, Go condition of OTp; OTe, Go condition of OTe (dashed lines as for the Go condition). OBSv, from left to right: grasping observation, pantomimed grasping, static frame of a grasping action, static frame of a pantomimed action, static frame with the target object. Color code indicates small (orange) and big (grey) object trials. Vertical dashed lines indicate, in the VMT, OTp and OTe (from left to right) the cue sound onset, object presentation, and sound off (Go/No-Go signal); triangular markers indicate movement onset (green), reward delivery (red). In OTv the dashed lines indicate the (dynamic or static) stimulus onset. (B) Example neuron classified as motor-related in the VMT. Conventions as in (A). (C) Example neuron classified as visual-related in the VMT. Conventions as in (A). (D) Example neuron classified as task unrelated in the VMT. Conventions as in (A).

static or dynamic (Fig. 1G), as well as of the target objects (small or big sphere) alone (see Fig. S1 for details on the number of correct and incorrect trials in VMT and OTs).

Based on the VMT, which is the type of task most widely used to characterize neuronal properties in parieto-frontal regions, we classified neurons as visuomotor (79/134, 58.9 %), visual related (26/134, 19.4 %), motor related (13/134, 9.7 %), and VMT-unrelated (16/134, 12 %), with similar fractions of neurons in each category in the two monkeys (Table S1). When tested in the OTs, only 4 of the 16 VMT-unrelated neurons turned out to be unrelated also to action observation, whereas all the remaining neurons modulated in the VMT also responded in the OTs, with different response pattern across action observation conditions (see Table 1).

Specifically, all but 3 of the 79 visuomotor neurons classified based

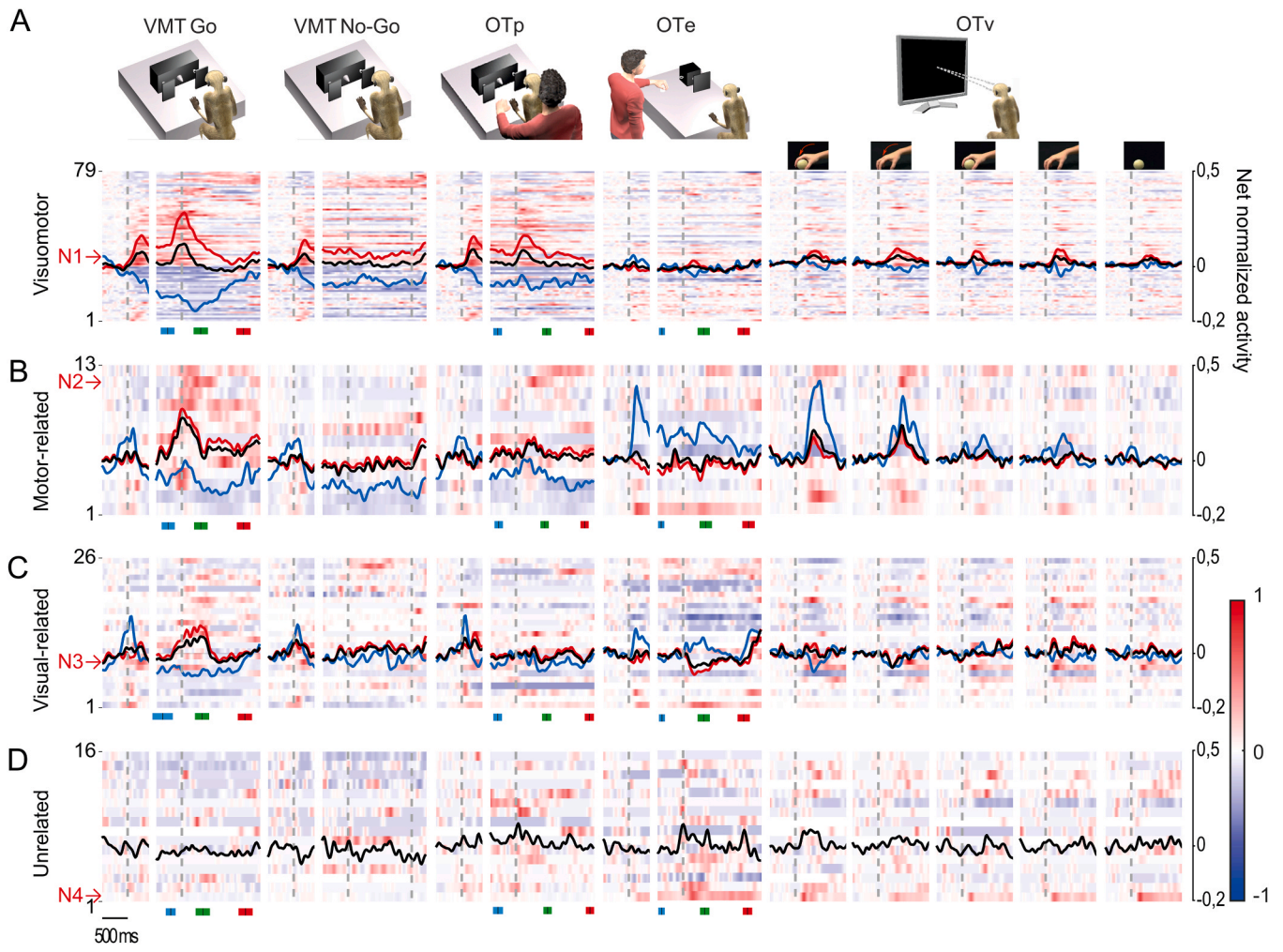

Fig. 3. Functional specificity of neurons classified based on the VMT. Schematic representation of each task as in Fig. 2. (A) Heatmaps and population response of visuomotor neurons: the red polyline represents the mean activity of the neuronal population facilitated during the VMT, whereas the blue one represents the suppressed neuronal population (black line is the average population response). Vertical dashed lines indicate, in the VMT, OTp, and OTe (from left to right) the object presentation, and movement onset (Go trials) or sound off (No-Go signal); in OTv the dashed lines indicate the (dynamic or static) stimulus onset. Neurons are sorted based on the timing of their facilitated or suppressed response in the VMT (earlier first), and the same order is maintained for all the other tasks to allow for comparison. Colored markers under each plot represent the average timing (± 1 STD) of occurrence of Go-signal (blue), pulling onset (green), and reward delivery (red). (B) Heatmaps and population response of motor-related neurons. Note that the two neurons suppressed during VMT (blue polyline) exhibited an overall facilitated response during action observation in OTe and OTv. (C) Heatmaps and population response of visual-related neurons. Note that six neurons are classified as suppressed (blue polyline) based on the activity during grasping execution in the light and they exhibited an overall facilitated response during object presentation in VMT, OTp, and OTe, but not OTv, whereas the remaining did only discharge during grasping in the light. (D) Heatmaps and population response of VMT-unrelated neurons. Note that among these neurons only 4 are unrelated also during the observation tasks, whereas the remaining 12 exhibited facilitated discharge during some of the observation tasks.

on the VMT also responded during the observation tasks, either only during live (23/79) or video (1/79) or, in most cases (52/79), to live and filmed actions (see example neuron in Fig. 2A). Interestingly, 11 out of the 13 neurons classified as motor-related with the VMT responded also during the observation of filmed and/or live actions during the observation tasks (see example neuron in Fig. 2B), indicating that they would have been misclassified as purely motor related solely based on the VMT. Among neurons classified as visual-related in the VMT because they did not respond during active execution of actions, most (14/26) responded to both live and filmed observed actions (see example neuron in Fig. 2C). Finally, eleven of the recorded neurons that did not show any significant response in the VMT nonetheless could respond during action observation (see example neuron in Fig. 2D).

At the population level, visuomotor neurons (n=79, Fig. 3A) include a sizeable fraction (n=28) of cells significantly suppressed during the reaching-grasping actions at least in the dark condition, whereas the majority (n=51) exhibited the typical visual-to-motor enhancement of activity reported by classical AIP studies with visuomotor tasks (Murata et al., 2000). Interestingly, many of these neurons also responded when the monkey observed another's action, particularly during the OTp and OTv. Motor-related neurons classified based on the VMT (Fig. 3B), can also respond during OTe and OTv, typically with increased activity, even in the case of neurons exhibiting suppressed modulation (2 out of 13) during action execution. Concerning the subpopulation of neurons with visual-related properties in the VMT (n=26), their response was present during object presentation and/or during object grasping, only in the light (Fig. 3C). Interestingly, all the six neurons classified as suppressed based on the activity during grasping execution in the light exhibited an overall facilitated response during object presentation in VMT, OTp, and OTe, but not OTv. Moreover, among the 20 neurons classified as facilitated in the VMT, some showed suppressed activity during the grasping epoch in OTe (n=8) and OTv (n=7); only one in OTp. Considering the last category, by definition unrelated neurons (n=16) did not show any modulation during VMT. However, the great majority of them (n=13)

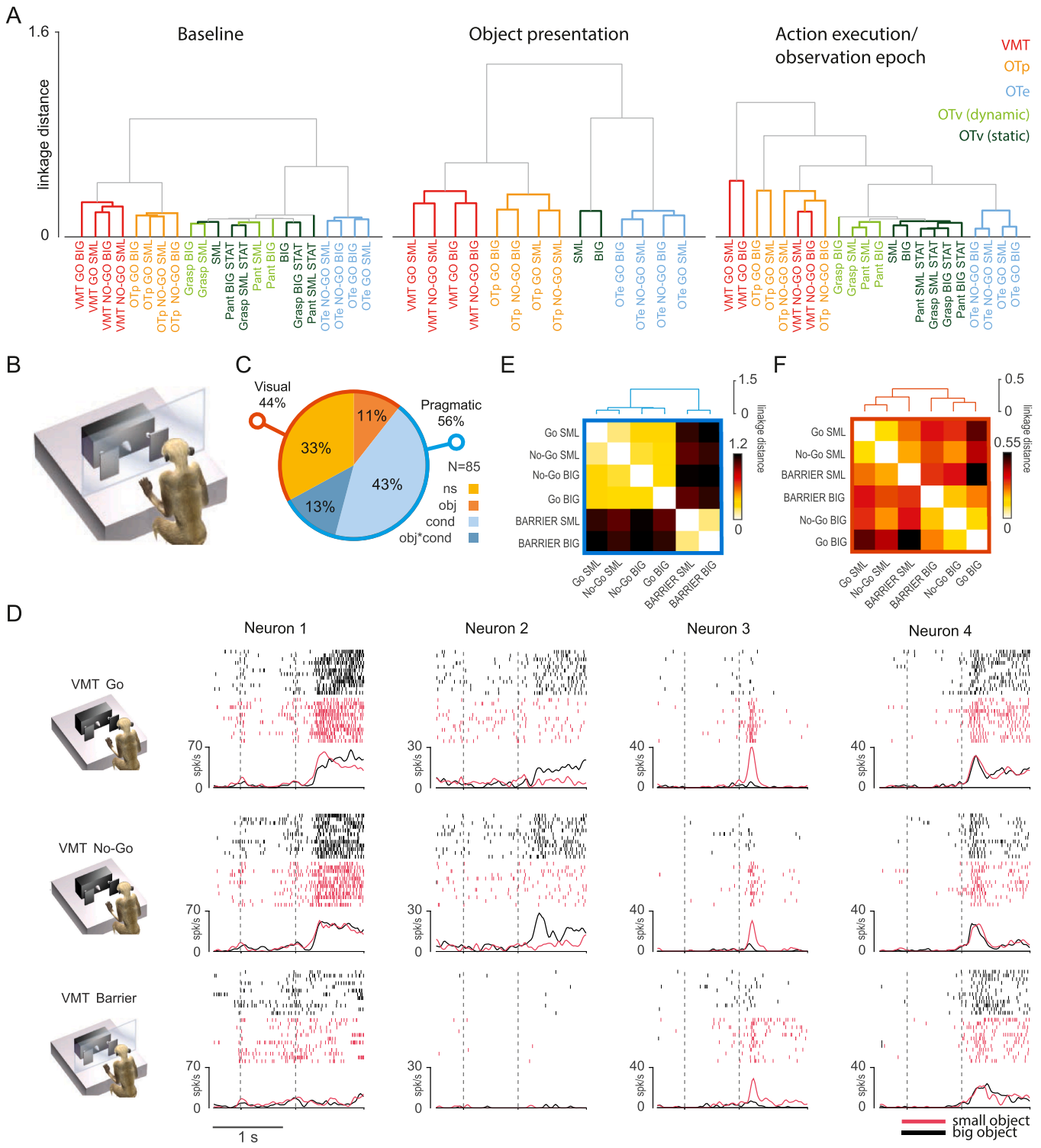

Fig. 4. Clustering of tasks and experimental conditions. (A) Dendrogram illustrating the neural distances between task conditions (color code) during baseline, object presentation, and action execution/observation. (B) Behavioral setting for the Barrier condition. (C) Pie chart representing the percentage of visually-responsive neurons exhibiting a significant effect of condition, alone or in interaction with object (56%, corresponding to pragmatic coding), object or none of the two factors (44%, corresponding to visual coding). (D) Example neurons showing a pragmatic (Neuron 1 and 2) or visual (Neuron 3 and 4) coding during object presentation. Vertical dashed lines indicate, from left to right, the cue sound onset and object presentation. (E) Dissimilarity matrix computed with the Mahalanobis distances among conditions calculated on the basis of the discharge of neurons exhibiting pragmatic coding of objects. (F) Dissimilarity matrix computed with the Mahalanobis distances among conditions calculated on the basis of the discharge of neurons exhibiting visual coding of objects.

Table 1
Responses in the Ots of all AIP neurons primarily classified based on their response properties in the VMT.

			Classification based on VMT				
			Visuomotor	Visual related	Motor related	Unrelated	
Classification based on OTs	Live	OTp	14	1	2	2	19
		OTe	4	3	0	2	9
		OTp and OTe	5	5	1	1	12
	Video	OTv	1	2	1	1	5
	Live and Video		52	14	7	6	79
	Unrelated		3	1	2	4	10
			79	26	13	16	134

showed significant modulation during the grasping epoch of at least one of the three Observation Tasks (Fig. 3D).

Altogether, the present findings indicate that by adopting a larger set of tasks and testing conditions, the classical distinction of AIP neurons into discrete categories appears too simplistic. Interestingly, even by applying an unbiased hierarchical clustering of AIP neurons based on their firing features in different conditions and epochs (Fig. S2), the findings reveal the presence of a limited number of remarkably distinct sets of cells that, nevertheless, are characterized by mixed selectivity for self and others' actions, as well as for observed objects, with a variety of complex, context-dependent modulations of their discharge.

Based on such heterogeneous firing features of AIP neurons in the various tasks and conditions, next we investigated the possible relationship between neural codes in the different tasks and epochs. To this purpose, we first applied a hierarchical cluster analysis by computing the Mahalanobis distances between each pair of conditions of interest in the complete neural state space and presented the clusters solutions for different epochs as dendrograms (Fig. 4A). Considering the baseline epoch, the linkage distances among tasks, which were run in blocks and hence known to the monkey since the beginning of each trial, indicate a first segregation between VMT and OTp, on one side, and OTe and OTv, on the other, suggesting that events occurring within or outside the monkey's working space may be processed differently by AIP neuronal activity. A further separation is observed between the two tasks within each of these subspaces. Note that these distances are greater than those between types of objects and Go/No-Go conditions, which are not yet known to the monkey at this initial stage of the task and their separation is therefore based on chance. During the object presentation epoch (Fig. 4B), the initial segregation increases, highlighting a further separation between small and big objects. The same clusters become even more marked during the movement phase in the dark, where the separation increases between the condition in which the monkey actively grasped a target and those in which it remained still, indicating that the neural distances are primarily influenced by motor rather than visual factors. Coherently, the distinction between the target objects is markedly evident when they are presented within the monkey's working space (i.e. in the Go and No-Go conditions of the VMT and in the OTp), but not when they are presented in the monkey's extrapersonal space (OTe) or on a screen (OTv).

The dichotomy between peri- and extra-personal space has been widely tested in premotor areas (Bonini et al., 2014; Lanzilotto et al., 2016; Caggiano et al., 2009), where pragmatic coding of objects and actions prevails, but not in area AIP. Furthermore, AIP is known to be highly sensitive to changes in visual features, which are unavoidably associated with stimuli presented on different media and/or at different distances, thus making impossible to distinguish between visual and pragmatic representation of objects in area AIP solely based on the testing conditions presented so far. To address this issue, we tested a sizeable fraction of the recorded neurons in a modified version of the Go condition of the VMT in which a transparent plastic barrier was interposed between the monkey's hand and the target objects, so that the absolute position and retinal image of the objects were exactly the same as in the VMT but their pragmatic relevance was different (Fig. 4B). By applying a 2 × 3 repeated measures ANOVA (factor: Object and Condition) we compared single neurons' response during object presentation in the Go, No-Go, and Barrier conditions. We found that most of visually responsive neurons showed a significant effect of the factor Condition (Fig. 4C), either as a main effect (n = 37, e.g. neuron 1 in Fig. 4D) or in interaction with the factor Object (n = 11, e.g. neuron 2 in Fig. 4D): these properties are in line with the pragmatic coding hypothesis. In contrast, a few neurons displayed pure selectivity for object regardless of the condition (n = 9, e.g. neuron 3 in Fig. 4D) and some exhibit a visual response with no selectivity (n = 28, e.g. neuron 4 in Fig. 4D): these properties are compatible with a purely visual coding. Mahalanobis distances calculated on these sets of neurons demonstrate that neurons with pragmatic coding properties distinguish the Barrier condition from the other visual presentation conditions, despite the retinal image of the objects was the same (Fig. 4E), whereas neurons with visual coding properties encode the objects regardless of the visual presentation condition (Fig. 4F).

3. Discussion

Some of the most widely established, textbook views on sensorimotor coding along the parieto-frontal circuits (Kandel et al., 2021) maintain that distinct categories of neurons, partially segregated along different pathways, subserve the transformation of the physical properties of observed objects into potential motor plans (i.e. the so-called "canonical neurons"), the encoding of their spatial position relative to the subject's body (i.e. the so-called "peripersonal neurons"), or the representation of observed actions of others (i.e. the so-called "mirror neurons"). The dichotomy between object and action coding operated by distinct neuronal categories has been already proven to be untenable in premotor areas (Bonini et al., 2014; Livi et al., 2019), where individual neurons can modulate their discharge during both object and action observation, with both types of responses often constrained to the monkey's peripersonal space (Maranesi et al., 2017; Albertini et al., 2021). The findings of the present study show that a shift in the classical view, which emphasizes the distinction between neuronal categories, is warranted for the parietal cortex as well.

Indeed, we have demonstrated that almost all (96 %) AIP neurons classified as "visuomotor" using a classical definition based on their visual and motor responses in a visuomotor task, did also respond to observed actions regardless of the format: live, filmed, or both. Conversely, less than 10 % of the neurons responding to other's actions (live, filmed, or both) exhibited pure selectivity for these types of stimuli: the overwhelming majority (more than 90 %) were generally modulated also during the sight of a target object or of one's own hand visual feedback during grasping. Thus, most of AIP neurons exhibit multiple and combined modulations during sensory and motor processing of objects and/or other's actions, suggesting that the classical approach based on pure selectivity for discrete variables is too

simplistic.

An additional element in AIP functioning, so far scarcely considered, is the contribution of neurons with suppressed modulation. Here, we showed that all subsets of AIP neurons (motor, visuomotor, and visual-related) include a variable proportion of cells with suppressed response during different conditions and epochs of the tasks (Fig. 2), in line with a previous study comparing different parieto-frontal areas (Ferroni et al., 2021). Furthermore, unsupervised hierarchical clustering (Fig. S2) revealed that the suppressed modulations are capable to segregate neuronal pools in AIP, suggesting that they constitute a crucial feature of parietal, in addition to frontal, areas. Interestingly, some cells showed an opposite pattern of activity during action execution and observation (e.g., facilitated-suppressed, or viceversa), as originally demonstrated in PMv (Kraskov et al., 2009), while other neurons, classified as visual-related based on the VMT and exhibiting facilitated response, often showed suppressed discharges during specific conditions of the OTs (i.e. OTe and OTv). Finally, even neurons classified as task unrelated in the VMT often showed stronger modulations, facilitated or suppressed, during the observation tasks, particularly OTp and OTe. The picture emerging from our data clearly indicates that monkey AIP displays mixed selectivity and complex modulations depending on different tasks and conditions. Nonetheless, it is possible to identify some general coding principles underlying different tasks, stimuli, and conditions, suggesting that partially mixed selectivity characterizes AIP functioning in non-human primates, as previously suggested in humans (Zhang et al., 2017) and in other parietal regions (Rishel et al., 2013; Vaccari et al., 2022).

Observing objects or another's action, both when contextual cues allow the observer to anticipate a forthcoming action (Go condition) or its absence (No-go condition), strongly modulates AIP neurons activity, as previously demonstrated in ventral (Bonini et al., 2014; Caggiano et al., 2009) and mesial (Livi et al., 2019) premotor cortex. Furthermore, the clustering of active vs. passive tasks during the baseline periods has been previously reported in studies with similar tasks carried out in the monkey mesial premotor cortex (Albertini et al., 2020). The potential to interact with the target also allows object coding to emerge, especially when the object is not only presented in the monkey's own workspace, but also targeted by the subsequent monkey's own action, such as during Go trials. Furthermore, the subjective viewpoint within the monkey's peripersonal space appears to be a crucial element to enhance AIP neurons' response, especially that of facilitated neurons, in line with previous neurophysiological studies in both AIP (Pani et al., 2014; Maeda et al., 2015) and the ventral premotor cortex (Bonini et al., 2014; Maranesi et al., 2017). Together, these findings suggest that in AIP, likewise in premotor cortex, an important representational principle underlying mixed selectivity is the pragmatic coding, that is, the encoding of the motor opportunities to act on, or interact with, the observed stimuli.

Nevertheless, it is also known that AIP neurons tend to exhibit a more marked tuning for 3d object properties, such as shape and orientation, relative to the premotor cortex, where neuronal activity distinguishes objects based on the hand shape required for grasping them rather than their visual features (Schaffelhofer and Scherberger, 2016). Thus, the pragmatic coding hypothesis needs to be directly tested in AIP because the above-mentioned differences may also constitute a byproduct of the unavoidable differences in retinal images of objects and actions across the experimental conditions (e.g. objects presented near of far from the monkey, or on a screen, project considerably different retinal images and are associated with highly different visual properties). Our results with the Barrier condition demonstrate that a set of AIP neurons responding to object presentation reflect a purely visual coding of object and/or their 3d features regardless of the experimental condition. In contrast, most of AIP visually responsive neurons are significantly modulated by the presence of a transparent barrier interposed between the monkey and the object, which does not alter the retinal image of the object but changes its pragmatic valence, thus indicating pragmatic coding. Coherently, the few available data concerning AIP inactivation indicate an impairment in the monkey's capacity to coordinate visually-guided actions toward graspable object (Gallese et al., 1994). Unfortunately, similar tests have never been done to explore a possible impairment in the capacity to plan actions directed to others, but recent multimodal lesion mapping and electrophysiological studies in human patients (Fornia et al., 2023) suggest that territories of the human rostral intraparietal sulcus, putative homologue of monkeys AIP, indexes a convergence of sensorimotor, praxis, and imitative skills.

In conclusion, the present findings support recently proposed perspectives (Orban et al., 2021a) maintaining that sensory information related to the actions of others and manipulable objects is processed by the same neuronal substrates, enabling to exploit neural codes for actions to plan potential motor responses to both the physical and social world.

4. Material and methods

Experiments were carried out on two *Macaca mulatta*, one female (Mk1 - 4 kg) and one male (Mk2 - 7 kg). Before recordings, monkeys were habituated to sit in a primate chair and to interact with the experimenters. They were then trained to perform a visuomotor task (VMT), and a variety of observation tasks, either live (OTp and OTe, see Bonini et al. (2014) and Maranesi et al. (2015) or involving filmed actions (OTv). When the training was completed, a head fixation system was implanted under deep sedation (ketamine hydrochloride, 5 mg/Kg i.m. and medetomidine hydrochloride, 0.1 mg/Kg i.m.), followed by postsurgical pain medications. Surgical procedures were the same as previously described (Bruni et al., 2017). All experimental protocols complied with the European (Directive 2010/63/EU) and national (Dlgs 26/2014) laws on the humane care and use of laboratory animals, they were approved by the Animal Welfare Body of the University of Parma and authorized by the Italian Ministry of Health.

4.1. Apparatus and behavioral paradigm

During the VMT, OTp, and OTe, the monkey was seated on a primate chair in front of a box (Fig. 1B, C, D) previously used in other experiments (Bonini et al., 2014), whereas during OTv it was sitting in front of a video monitor (Fig. 1E). The tasks were carried out in distinct, subsequent blocks during the same recording session.

The VMT was performed by using a box divided horizontally into two sectors by a half-mirror: the upper sector contained a small black tube with a white light-emitting diode (LED) that could project a spot of light on the half-mirror surface; the lower sector contained a sliding plane hosting three different objects. When the LED was turned on (in complete darkness), the half-mirror reflected the spot of light so that it appeared to the monkey as located in the lower sector (fixation point), in the position of the center of mass of the not-yet-visible target object. The objects – a small and a large cone – were chosen because they afforded two different grip types: side grip (performed by opposing the thumb and the lateral surface of the index finger) and whole-hand prehension (achieved by opposing all the fingers to the palm). Objects were randomly presented through a 7 cm opening located on the monkey's sagittal plane, at a reaching distance from the starting position of the monkey's hand. A stripe of white LEDs located on the lower sector of the box allowed us to illuminate objects during specific phases of the task. Note that, because of the half-mirror, the fixation point remained visible in the middle of the object even when the lower sector of the box was illuminated.

The VMT included three fully randomized conditions, as illustrated in Fig. 1F: grasping in the light, grasping in the dark and a no-go condition. Each of them started when the monkey held its hand on a starting button, after a variable inter-trial period ranging from 1 to 1.5 seconds from the end of the previous trial. The fixation point was presented and the monkey was required to gaze at the fixation point within 1.2 s.

Fixation onset resulted in the presentation of a cue sound (Go-cue, a pure high tone constituted by a 1200 Hz sine wave for grasping in the light and grasping in the dark; No-go cue, a pure low tone constituted by a 300 Hz sine wave for the No-go condition), which instructed the monkey to grasp the subsequently presented object (Go condition) or to keep the hand still on the starting position (No-go condition). After 0.8 s the lower sector of the box was illuminated and one of the objects became visible. Then, after a variable time lag (0.8–1.2 s), the sound ceased (Go-signal/No-go signal), and the monkey had to reach, grasp and pull the object within 1.2 s (holding it steadily for 0.8 s) or to keep the hand on the starting position. During the Grasping in the dark condition, when the cue sound ceased (go signal), the light inside the box automatically switched off and the monkey performed the subsequent motor acts in complete darkness. The fixation point was visible for the entire duration of each trial, providing a spatial guidance for reaching the object in the absence of visual feedback. In this paradigm, grasping in the light and grasping in the dark trials were identical and unpredictable until the occurrence of the go signal, to ensure that action planning was the same in both conditions. In all conditions, the monkey had to maintain fixation along all the trial. At the end of each correctly performed trial, the reward (a drop of juice) was automatically delivered. We collected 12 correctly performed trials for each condition and with each object.

An additional condition (Barrier) was carried out on a consistent number of neurons (3 sessions, n = 119): the same sequence of events of the No-Go condition was employed in the presence of a transparent plastic barrier interposed between the monkey's hand and the target, and the go-cue sound ensure that the monkey refrained from acting because of the presence of the barrier (Lanzilotto et al., 2016).

The OTp and OTe were based on the same sequence of events and temporal constraints as in the monkey VMT. In particular, the experimenter performed two conditions (grasping in the light and the No-go condition) in a randomized order, while the monkey had to simply maintain fixation and keep the hand on the starting position to get the reward, in both tasks.

The OTv was performed with the monkey facing a video monitor (1920 × 1080, 60 Hz). The monitor was located 57 cm from the monkeys' face, and the video took up an area of 13.04° x 9.85° of the visual field in the horizontal and vertical dimension, respectively. Videos of different grasping or mimicked grasping were presented: actions were performed with a small or a big sphere as a target (Grasping condition) or with no object (Pantomime condition). Stimuli included also video presenting static images obtained from 1) the presentation of the object alone, 2) the first frame of contact between the hand and the object (Grasping condition), and 3) the corresponding period of the mimicked grasping without the object (Pantomime). First, the monkey had to gaze at a red square on a black background. Then, the video stimulus started and lasted 1.5 s. The monkey was required to remain still, with its hand on the starting position, and to maintain fixation (within a 3° spatial window centered on the fixation point) for the entire duration of the trial. The reward was automatically delivered at the end of each correctly performed trial. The stimuli were randomly presented and a total of 12 correct trials for each stimulus type were collected.

The phases of all tasks were automatically controlled and monitored by LabView-based software, enabling the interruption of the trial if the monkey broke fixation, made an incorrect movement, or did not respect the task temporal constraints described above. In all these cases, no reward was delivered. After correct completion of a trial, the monkey was automatically rewarded with the same amount of juice in all conditions (pressure reward delivery system, Crist Instruments, Hagerstown, MD).

4.2. Recording techniques

Neuronal recordings were performed by means of chronically implanted arrays of linear silicon probes with 32 recording channels per shaft. Probes were implanted by estimating the angle of penetration with MRI-based reconstruction of the outline of the intraparietal sulcus at the selected site of insertion (see Fig. 1A). Previous reports provide more details on the methodology of probe fabrication, assembly and implantation (Bonini et al., 2014; Barz et al., 2014; Herwik et al., 2011), as well as on probes' recording performance over time in chronic applications (Barz et al., 2017). After the recordings, the location of the recorded region was histologically confirmed post-mortem (Lanzilotto et al., 2019).

The neural signal was amplified and sampled at 30 kHz with four 32-channel Intan amplifier boards (Intan Technologies, Los Angeles, CA, USA), controlled in parallel via the electrophysiology platform Open Ephys (http://open-ephys.org/). Spike sorting was performed off-line with fully automated software, Mountainsort (Chung et al., 2017), with a threshold of −3.0 standard deviations of the signal-to-noise ratio for each channel for detecting units. To distinguish single- from multi-unit we set the noise overlap, a parameter that can vary between 0 and 1, with a value below 0.1 for single units. Single unit isolation was further verified using standard criteria (ISI distribution, refractory period > 1 ms, and absence of cross-correlated firing with time-lag of ≈ 0 relative to other isolated units, to avoid oversampling), possible artifacts were removed, and all the remaining waveforms that could not be classified as single units formed the multiunit activity.

4.3. Recording of behavioral events and definition of epochs of interest

Distinct contact sensitive devices (Crist Instruments) were used to detect when the monkey's and the experimenter's hand (grounded) touched the metal surface of the starting button or one of the target objects. To signal the onset and tonic phase of object pulling, an additional device was connected to the switch located behind each object. Each of these devices provided a TTL signal, which was used by the LabView-based software to monitor the monkey's performance and to control the generation and presentation of the behavioral paradigm's auditory and visual cue signals.

Eye position was monitored in parallel with neuronal activity with an eye tracking system consisting of a 50 Hz CCD video camera provided with an infrared filter and two spots of infrared light. Two identical but independent systems were used for monitoring eye position during all tasks. Analog signal related to horizontal and vertical eye position was fed to a computer equipped with dedicated software, enabling calibration and basic processing of eye position signals. The same software also generated different digital output signals associated with various input and output events of all the tasks. These signals were recorded and stored together with the neuronal activity and subsequently used to construct the response histograms and the data files for statistical analysis.

Unit activity was analyzed in relation to the digital signals associated with the main behavioral events. In the VMT we considered the following epochs of interest: 1) baseline, 500 ms before object presentation; 2) object presentation, from 0 to 500 ms after switching on the light; 3) premovement, 500 ms before reaching-grasping onset (detachment of monkey's hand from the starting position); 4) reaching-grasping, from reaching onset to pulling onset (of variable duration, calculated on a trial-by-trial basis); 5) object holding, from pulling onset to 500 ms after this event. Note that during baseline the monkey had its hand still on the starting button, it was staring at the fixation point, and since the cue sound was playing it was already aware of whether the ongoing trial was a go or a no-go trial.

In the OTp and OTe the temporal sequence of task events was the same of the VMT, thus, we considered the same epochs of interest. In the OTv the epochs of interest were the following: 1) baseline, 500 ms before stimulus presentation onset; 2) stimulus presentation, from the onset of the (static or dynamic) stimulus to 1 second after this event. Five different stimuli could be presented during epoch 2: 1) the static frame of the small or big object; 2) a grasping action with precision or power grip; 3) a mimicked precision grip or power grip in the absence of

the object; 4) the static frame of the hand-object interaction with the small or big object, and 5) a static frame of the mimicked precision or power grip in the absence of the object.

4.4. Data analyses

Single -unit classification. Single units were primarily classified based on their response in the VMT in the epochs of interest described above relative to baseline as facilitated (when the response was significantly stronger than baseline) or suppressed (when the response was weaker than baseline). Object presentation response was assessed by means of a 2 × 2 x 2 repeated measures ANOVA with the factors Object (small and big), Condition (Go and No-Go), and Epoch (baseline, object presentation). To investigate the possible pragmatic relevance of objects in AIP, we tested neurons recorded in the Barrier condition during object presentation by means of a 2 × 3 repeated measures ANOVA with the factors Object (small and big) and Condition (Go, No-Go and Barrier). The possible modulation during premovement, reaching-grasping, and object holding epochs relative to baseline was analyzed by means of a two 2 × 4 repeated measures ANOVA (factors: Object and Epoch), carried out in grasping-in-the-light and grasping-in-the-dark trials, separately. When neurons showed modulation during both grasping-in-the-light and grasping-in-the-dark, we assessed the possible difference between the two conditions by means of a 2 × 2 x 3 repeated measures ANOVA (factors: Object, Condition and Epoch). All ANOVAs were carried out with a significant criterion of $P < 0.05$ and followed by Bonferroni post-hoc tests ($p < 0.05$) in the case of significant interaction effects or to identify main effects of factors with more than 2 levels.

The neurons classification was based on the possible difference between neuronal activity during task-related epochs (object presentation and the four motor epochs) and baseline. We classified as motor-related those neurons with no modulation during object presentation, showing a significant effect ($p < 0.05$) of the factor Epoch (as a main effect or in interaction with the factor Object) both in the dark and in the light and with no significantly different discharge between these two conditions. Visual-related neurons discharged significantly either during at least one of the four motor epochs of grasping in-the-light but not in the dark, and/or during object presentation. We classified as visuomotor neurons those cells discharging during object presentation and during one of the four motor epochs of grasping in the dark, in addition to those neurons discharging only during at least one of the four motor epochs of the VMT but differently between light and dark conditions. Finally, neurons with no modulation in any epoch relative to baseline were classified as VMT unrelated.

Heat Maps Construction. Heat maps have been built to show the temporal activation profile of individual neurons in the neuronal population categories in each task. Each line represents the activity of a single unit averaged across 24 trials with the two different objects, averaged ($n = 12$ for each object). The color code represents the net normalized activity, computed as follows: for each neuron, a mean baseline value across the 24 trials was computed (500 ms before object presentation), and then subtracted bin-by-bin for the entire task period. Activity was aligned to the object presentation and movement onset. Finally, the net activity was normalized to the absolute maximum bin value (in each individual cell) across the conditions. All final plots were performed using a bin size of 100 ms and steps of 20 ms.

Hierarchiacal cluster analysis. To evidence the possible relationship among neural representations of tasks and conditions, we performed a hierarchical cluster analysis. Given a certain neural population including N units, the firing rates of all units were calculated by binning their spiking activity and averaging it across trials. We created a firing rate matrix F with N rows and c*t columns (where c is the number of conditions and t the number of time points per condition within the epoch of interest). Then, we computed the Mahalanobis linkage distances (Matlab function: manova1) between the activities in the N-dimensional state space of all possible pairs of conditions in the epoch of interest. Since the Mahalanobis distance between any pair of arbitrarily selected conditions increases linearly as a function of the number of units in the population, the resulting matrix of distances was normalized dividing it by N. Finally, normalized distance matrix was used to create a hierarchical cluster tree based on the average linkage criterion (Matlab function: manovacluster), presenting the cluster solutions in the form of dendrograms. While building the dendrograms, we sorted the leafs within a branch based on their average distance to nearest branches (Matlab function: optimalleaforder).

Unsupervised hierarchical clustering. To further test for mixed selectivity in the population with no a priori classification of neurons, an unsupervised hierarchical cluster analysis was performed using the mean net firing rate of each neuron calculated in 14 different epochs of interest across tasks: object presentation (VMT go trials), reaching-grasping in the light, reaching-grasping in the dark, object presentation (VMT no-go trials), No-go signal (VMT), object presentation (OTp go trials), reaching-grasping (OTp go trials), object presentation (OTe go trials), reaching-grasping (OTe go trials), and stimulus presentation in the 5 conditions of OTv. The analysis was implemented by using the *hcpc* function in the FactoMineR package in R (Lê et al., 2008), which first creates a hierarchical tree based on Ward's method for hierarchical agglomerative clustering (Ward Jr.., 1963), and then estimates the optimal number of clusters by calculating the partition with the higher relative loss of inertia (i.e., 'error sum of square') (Randriamihamison et al., 2021). The clusters obtained were used to plot a heatmap of the data (i.e., the neurons' mean net activity in the epoch of interest).

CRediT authorship contribution statement

Luca Bonini: Writing – review & editing, Writing – original draft, Methodology, Funding acquisition, Conceptualization. **Edoardo Arcuri:** Writing – review & editing, Formal analysis. **Marco Lanzilotto:** Writing – review & editing, Investigation, Conceptualization. **Monica Maranesi:** Writing – review & editing, Writing – original draft, Methodology, Investigation, Formal analysis, Conceptualization.

Declaration of Competing Interest

The authors declare no competing interests.

Data availability

Data will be made available on request.

Acknowledgements

The work was supported by #NEXTGENERATIONEU (NGEU) and funded by the Ministry of University and Research (MUR), National Recovery and Resilience Plan (NRRP), project MNESYS (PE0000006) – A Multiscale integrated approach to the study of the nervous system in health and disease (DN. 1553 11.10.2022); ERC Stg-2015 678307 (WIRELESS); ERC CoG-2020 101002704 (EMACTIVE). ML is supported by BBRF 2021 Young Investigator Grant (Grant ID: 30604).

Author contributions

Conceptualization, M.M, M.L., and L.B; Investigation, M.M, M.L., and L.B; Formal Analysis, M.M and E.A.; Writing - Original Draft, M.M. and L.B; Writing - Review & Editing, M.M., M.L., E.A., L.B.

Appendix A. Supporting information

Supplementary data associated with this article can be found in the online version at doi:10.1016/j.pneurobio.2024.102611.

References

Albertini, D., Gerbella, M., Lanzilotto, M., Livi, A., Maranesi, M., Ferroni, C.G., Bonini, L., 2020. Connectional gradients underlie functional transitions in monkey pre-supplementary motor area. Prog. Neurobiol. *184*, 101699 https://doi.org/10.1016/j.pneurobio.2019.101699.

Albertini, D., Lanzilotto, M., Maranesi, M., Bonini, L., 2021. Largely shared neural codes for biological and nonbiological observed movements but not for executed actions in monkey premotor areas. J. Neurophysiol. *126* (3), 906–912. https://doi.org/10.1152/jn.00296.2021.

Barz, F., Livi, A., Lanzilotto, M., Maranesi, M., Bonini, L., Paul, O., Ruther, P., 2017. Versatile, Modular 3D microelectrode arrays for neuronal ensemble recordings: from design to fabrication, assembly, and functional validation in non-human primates. J. Neural Eng. *14* (3), 036010 https://doi.org/10.1088/1741-2552/aa5a90.

Barz, F.; Paul, O.; Ruther, P. Modular Assembly Concept for 3D Neural Probe Prototypes Offering High Freedom of Design and Alignment Precision. Annu. Int. Conf. IEEE Eng. Med. Biol. Soc. IEEE Eng. Med. Biol. Soc. Annu. Int. Conf. 2014, *2014*, 3977–3980. https://doi.org/10.1109/EMBC.2014.6944495.

Baumann, M.A., Fluet, M.-C., Scherberger, H., 2009. Context-specific grasp movement representation in the macaque anterior intraparietal area. J. Neurosci. *29* (20), 6436–6448. https://doi.org/10.1523/JNEUROSCI.5479-08.2009.

Bonini, L., Maranesi, M., Livi, A., Fogassi, L., Rizzolatti, G., 2014. Space-dependent representation of objects and other's action in monkey ventral premotor grasping neurons. J. Neurosci. *34* (11), 4108–4119. https://doi.org/10.1523/JNEUROSCI.4187-13.2014.

Bonini, L., Rotunno, C., Arcuri, E., Gallese, V., 2022. Mirror neurons 30 years later: implications and applications. Trends Cogn. Sci. *26* (9), 767–781. https://doi.org/10.1016/j.tics.2022.06.003.

Borra, E., Belmalih, A., Calzavara, R., Gerbella, M., Murata, A., Rozzi, S., Luppino, G., 2008. Cortical connections of the macaque anterior intraparietal (AIP) area. Cereb. Cortex 1991 *18* (5), 1094–1111. https://doi.org/10.1093/cercor/bhm146.

Bruner, E., 2018. Human paleoneurology and the evolution of the parietal cortex. Brain Behav. Evol. *91* (3), 136–147. https://doi.org/10.1159/000488889.

Bruni, S., Giorgetti, V., Fogassi, L., Bonini, L., 2017. Multimodal encoding of goal-directed actions in monkey ventral premotor grasping neurons. Cereb. Cortex 1991 *27* (1), 522–533. https://doi.org/10.1093/cercor/bhv246.

Buxbaum, L.J., Randerath, J., 2018. Limb apraxia and the left parietal lobe. Handb. Clin. Neurol. *151*, 349–363. https://doi.org/10.1016/B978-0-444-63622-5.00017-6.

Caggiano, V., Fogassi, L., Rizzolatti, G., Thier, P., Casile, A., 2009. Mirror neurons differentially encode the peripersonal and extrapersonal space of monkeys. Science *324* (5925), 403–406. https://doi.org/10.1126/science.1166818.

Chung, J.E., Magland, J.F., Barnett, A.H., Tolosa, V.M., Tooker, A.C., Lee, K.Y., Shah, K. G., Felix, S.H., Frank, L.M., Greengard, L.F., 2017. A fully automated approach to spike sorting. Neuron *95* (6), 1381–1394.e6. https://doi.org/10.1016/j.neuron.2017.08.030.

Ferroni, C.G., Albertini, D., Lanzilotto, M., Livi, A., Maranesi, M., Bonini, L., 2021. Local and system mechanisms for action execution and observation in parietal and premotor cortices. S0960-9822 Curr. Biol. CB (21), 00547. https://doi.org/10.1016/j.cub.2021.04.034.

Fornia, L., Leonetti, A., Puglisi, G., Rossi, M., Viganò, L., Della Santa, B., Simone, L., Bello, L., Cerri, G., 2023. The parietal architecture binding cognition to sensorimotor integration: a multimodal causal study. awad316 Brain J. Neurol.. https://doi.org/10.1093/brain/awad316.

Gallese, V., Murata, A., Kaseda, M., Niki, N., Sakata, H., 1994. Deficit of hand preshaping after muscimol injection in monkey parietal cortex. Neuroreport *5* (12), 1525–1529. https://doi.org/10.1097/00001756-199407000-00029.

Herwik, S., Paul, O., Ruther, P., 2011. Ultrathin silicon chips of arbitrary shape by etching before grinding. J. Micro Syst. *20* (4), 791–793. https://doi.org/10.1109/JMEMS.2011.2148159.

Intveld, R.W., Dann, B., Michaels, J.A., Scherberger, H., 2018. Neural coding of intended and executed grasp force in macaque areas AIP, F5, and M1. Sci. Rep. *8* (1), 17985 https://doi.org/10.1038/s41598-018-35488-z.

Kaas, J.H., Qi, H.-X., Stepniewska, I., 2018. The evolution of parietal cortex in primates. Handb. Clin. Neurol. *151*, 31–52. https://doi.org/10.1016/B978-0-444-63622-5.00002-4.

Kandel, E.R., Koester, J.D., Mack, S.H., Siegelbaum, S.A., 2021. Principles of Neural Science. McGraw Hill, pp. 815–859.

Kraskov, A., Dancause, N., Quallo, M.M., Shepherd, S., Lemon, R.N., 2009. Corticospinal neurons in macaque ventral premotor cortex with mirror properties: a potential mechanism for action suppression? Neuron *64* (6), 922–930. https://doi.org/10.1016/j.neuron.2009.12.010.

Lanzilotto, M., Ferroni, C.G., Livi, A., Gerbella, M., Maranesi, M., Borra, E., Passarelli, L., Gamberini, M., Fogassi, L., Bonini, L., Orban, G.A., 2019. Anterior intraparietal area: a hub in the observed manipulative action network. Cereb. Cortex *1991*. https://doi.org/10.1093/cercor/bhz011.

Lanzilotto, M., Livi, A., Maranesi, M., Gerbella, M., Barz, F., Ruther, P., Fogassi, L., Rizzolatti, G., Bonini, L., 2016. Extending the cortical grasping network: pre-supplementary motor neuron activity during vision and grasping of objects. Cereb. Cortex *26* (12), 4435–4449. https://doi.org/10.1093/cercor/bhw315.

Lanzilotto, M., Maranesi, M., Livi, A., Ferroni, C.G., Orban, G.A., Bonini, L., 2020. Stable readout of observed actions from format-dependent activity of monkey's anterior intraparietal neurons. Proc. Natl. Acad. Sci. *117* (28), 16596–16605. https://doi.org/10.1073/pnas.2007018117.

Lê, S., Josse, J., Husson, F., 2008. FactoMineR: an R package for multivariate analysis. J. Stat. Softw. *25* (1), 18. https://doi.org/10.18637/jss.v025.i01.

Lehmann, S.J., Scherberger, H., 2013. Reach and gaze representations in macaque parietal and premotor grasp areas. J. Neurosci. J. Soc. Neurosci. *33* (16), 7038–7049. https://doi.org/10.1523/JNEUROSCI.5568-12.2013.

Livi, A., Lanzilotto, M., Maranesi, M., Fogassi, L., Rizzolatti, G., Bonini, L., 2019. Agent-based representations of objects and actions in the monkey pre-supplementary motor area. Proc. Natl. Acad. Sci. *116* (7), 2691–2700. https://doi.org/10.1073/pnas.1810890116.

Maeda, K., Ishida, H., Nakajima, K., Inase, M., Murata, A., 2015. Functional properties of parietal hand manipulation–related neurons and mirror neurons responding to vision of own hand action. J. Cogn. Neurosci. *27* (3), 560–572. https://doi.org/10.1162/jocn_a_00742.

Maranesi, M., Bonini, L., Fogassi, L., 2014. Cortical processing of object affordances for self and others' action. Front. Psychol. *5*, 538. https://doi.org/10.3389/fpsyg.2014.00538.

Maranesi, M., Livi, A., Bonini, L., 2015. Processing of own hand visual feedback during object grasping in ventral premotor mirror neurons. J. Neurosci. *35* (34), 11824–11829. https://doi.org/10.1523/JNEUROSCI.0301-15.2015.

Maranesi, M., Livi, A., Bonini, L., 2017. Spatial and viewpoint selectivity for others' observed actions in monkey ventral premotor mirror neurons. Sci. Rep. *7* (1), 8231. https://doi.org/10.1038/s41598-017-08956-1.

Murata, A., Gallese, V., Kaseda, M., Sakata, H., 1996. Parietal neurons related to memory-guided hand manipulation. J. Neurophysiol. *75* (5), 2180–2186. https://doi.org/10.1152/jn.1996.75.5.2180.

Murata, A., Gallese, V., Luppino, G., Kaseda, M., Sakata, H., 2000. Selectivity for the shape, size, and orientation of objects for grasping in neurons of monkey parietal area AIP. J. Neurophysiol. *83* (5), 2580–2601. https://doi.org/10.1152/jn.2000.83.5.2580.

Orban, G.A., 2016. Functional definitions of parietal areas in human and non-human primates. Proc. Biol. Sci. *283* (1828), 20160118. https://doi.org/10.1098/rspb.2016.0118.

Orban, G.A., Lanzilotto, M., Bonini, L., 2021a. From observed action identity to social affordances. Trends Cogn. Sci. *25* (6), 493–505. https://doi.org/10.1016/j.tics.2021.02.012.

Orban, G.A., Sepe, A., Bonini, L., 2021b. Parietal maps of visual signals for bodily action planning. Brain Struct. Funct. *226* (9), 2967–2988. https://doi.org/10.1007/s00429-021-02378-6.

Pani, P., Theys, T., Romero, M.C., Janssen, P., 2014. Grasping execution and grasping observation activity of single neurons in the macaque anterior intraparietal area. J. Cogn. Neurosci. *26* (10), 2342–2355. https://doi.org/10.1162/jocn_a_00647.

Patri, J.-F., Cavallo, A., Pullar, K., Soriano, M., Valente, M., Koul, A., Avenanti, A., Panzeri, S., Becchio, C., 2020. Transient disruption of the inferior parietal lobule impairs the ability to attribute intention to action. Curr. Biol. CB *30* (23), 4594–4605.e7. https://doi.org/10.1016/j.cub.2020.08.104.

Randriamihamison, N., Vialaneix, N., Neuvial, P., 2021. Applicability and interpretability of ward's hierarchical agglomerative clustering with or without contiguity constraints. J. Classif. *38* (2), 363–389. https://doi.org/10.1007/s00357-020-09377-y.

Rishel, C.A., Huang, G., Freedman, D.J., 2013. Independent category and spatial encoding in parietal cortex. Neuron *77* (5), 969–979. https://doi.org/10.1016/j.neuron.2013.01.007.

Rizzolatti, G., Luppino, G., 2001. The cortical motor system. Neuron *31* (6), 889–901. https://doi.org/10.1016/s0896-6273(01)00423-8.

Romero, M.C., Janssen, P., 2016. Receptive field properties of neurons in the macaque anterior intraparietal area. J. Neurophysiol. *115* (3), 1542–1555. https://doi.org/10.1152/jn.01037.2014.

Romero, M.C., Pani, P., Janssen, P., 2014. Coding of shape features in the macaque anterior intraparietal area. J. Neurosci. *34* (11), 4006–4021. https://doi.org/10.1523/JNEUROSCI.4095-13.2014.

Romero, M.C., Van Dromme, I., Janssen, P., 2012. Responses to two-dimensional shapes in the macaque anterior intraparietal area. Eur. J. Neurosci. *36* (3), 2324–2334. https://doi.org/10.1111/j.1460-9568.2012.08135.x.

Sakata, H., Taira, M., Murata, A., Mine, S., 1995. Neural mechanisms of visual guidance of hand action in the parietal cortex of the monkey. Cereb. Cortex 1991 *5* (5), 429–438. https://doi.org/10.1093/cercor/5.5.429.

Schaffelhofer, S., Scherberger, H., 2016. Object vision to hand action in macaque parietal, premotor, and motor cortices. eLife *5*. https://doi.org/10.7554/eLife.15278.

Theys, T., Pani, P., van Loon, J., Goffin, J., Janssen, P., 2013. Three-dimensional shape coding in grasping circuits: a comparison between the anterior intraparietal area and ventral premotor area F5a. J. Cogn. Neurosci. *25* (3), 352–364. https://doi.org/10.1162/jocn_a_00332.

Theys, T., Srivastava, S., van Loon, J., Goffin, J., Janssen, P., 2012. Selectivity for three-dimensional contours and surfaces in the anterior intraparietal area. J. Neurophysiol. *107* (3), 995–1008. https://doi.org/10.1152/jn.00248.2011.

Vaccari, F.E., Diomedi, S., Filippini, M., Hadjidimitrakis, K., Fattori, P., 2022. New insights on single-neuron selectivity in the era of population-level approaches. Front. Integr. Neurosci. *16*, 929052 https://doi.org/10.3389/fnint.2022.929052.

Vallar, G., Calzolari, E., 2018. Unilateral spatial neglect after posterior parietal damage. Handb. Clin. Neurol. *151*, 287–312. https://doi.org/10.1016/B978-0-444-63622-5.00014-0.

Verhoef, B.-E., Michelet, P., Vogels, R., Janssen, P., 2015. Choice-related activity in the anterior intraparietal area during 3-d structure categorization. J. Cogn. Neurosci. *27* (6), 1104–1115. https://doi.org/10.1162/jocn_a_00773.

Ward Jr, J.H., 1963. Hierarchical grouping to optimize an objective function. J. Am. Stat. Assoc. *58* (301), 236–244. https://doi.org/10.1080/01621459.1963.10500845.

Zhang, C.Y., Aflalo, T., Revechkis, B., Rosario, E.R., Ouellette, D., Pouratian, N., Andersen, R.A., 2017. Partially mixed selectivity in human posterior parietal association cortex. Neuron *95* (3), 697–708.e4. https://doi.org/10.1016/j.neuron.2017.06.040.